

# Modeling & SMC Based Trajectory Tracking for a Tilt-Rotor Convertible UAV

Mohamed Zakaria Mimouni, Oualid Araar, Abdelkader Ouadda and Moussa Haddad  
*Ecole Militaire Polytechnique, Algeria*

**Keywords:** Tilt-Rotor UAV, SMC Control, Convertible UAV, Trajectory Tracking.

**Abstract:** Convertible UAVs combine the vertical takeoff and landing (VTOL) capabilities of multi-rotors with the endurance and high speed of fixed-wing drones. This work is concerned with a particular category of convertible UAVs, commonly termed Tilt-rotor UAVs (TRUAVs). First, a detailed dynamic model for a Quad-TRUAV is developed. This model features strong non-linearities and coupling, making its control a challenging task. The second contribution of this work is the design of a sliding mode controller (SMC) to ensure trajectory tracking. Simulations conducted on the full non-linear model of the famous Zagi-wing UAV show very promising results.

## 1 INTRODUCTION

Unmanned aerial vehicles (UAVs) have a wide range of military and civilian applications. These include infrastructure inspection, search and rescue, data collection (Li et al., 2021) delivery services, agriculture (Kim et al., 2019) and surveillance, to name but a few (Shakhatreh et al., 2019).

Convertible or Hybrid UAVs is a particular class, which has attracted considerable attention during the last few years. Hybrid designs target to combine the advantages of VTOL UAVs and those of the fixed wing category. These include high payload capacity, great operational range, high cruise speed, in addition to the stationary flight and VTOL capabilities.

Depending on their switching mechanism, convertible UAVs can be categorised into three main categories. The first includes tilt-rotors, which tilt their rotors to switch between VTOL and cruise flight modes. The second is tilt-wing in which the drone tilts both rotors and wings for switching. In the third category, named tail-sitters or tilt-bodies, the entire airframe is tilted for transitioning between flight modes.

The Tiltrotor UAV (TRUAV) is a very popular class of hybrid UAVs, in which the mounted rotors gradually tilt in the direction of flight, driving the aircraft forward until steady flight is reached (Saeed et al., 2015) (Hegde et al., 2019). This class is characterized by a simple transition manoeuvre and good controllability and stability (Saeed et al., 2018).

The TRUAV considered in this work is actuated

using only propellers, i.e it contains no control surfaces. In such a category, the tilting of the rotors results in considerable changes in the drone's center of gravity and moment of inertia (Su et al., 2019). It also results in rapid variations in the aerodynamic forces acting on the vehicle while changing from hover to cruise flight (Phung and Morin, 2014). These challenges complicate the dynamic model of the drone and hence its control (Ducard and Allenspach, 2021).

Among research works which have dealt with the control of TRUAVs, Papachristos et al. (Papachristos et al., 2013) developed a linear quadratic (LQ) control scheme for position control of a Three-Rotor TRUAV. In the hover phase, they implemented and experimentally tested PD & double Derivative controller (Papachristos et al., 2012).

In order to stabilize the pitch angle of a Three-Rotor TRUAV, Ta et al. (Ta et al., 2012) combined a linear PID controller and a nonlinear saturated sigmoid function. For the position, the authors employed a neural network-based adaptive controller. The proposed controller, however, does not account for the cross-coupling between states.

Flores et al. (Flores et al., 2012) applied a nonlinear backstepping controller for cruise flight. In hover mode, the TRUAV was controlled as a conventional multirotor using a feedback linearization technique.

In another work (Flores and Lozano, 2013), Flores et al. proposed a control solution to deal with the transition phase. The desired altitude was maintained

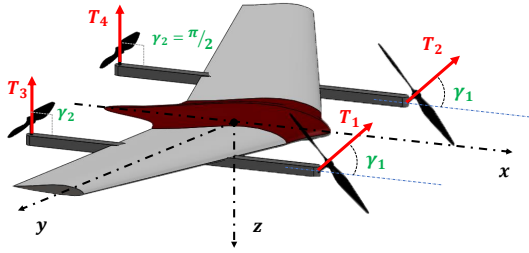


Figure 1: Illustration of the Quad-TRUAV considered in this work.

using nested saturation control. The input control vector includes elevator deflection, tilt angle, total rotor thrust, and difference in thrust between the front and rear rotors.

Hernandez-Garcia et al.(Hernandez-Garcia and Rodriguez-Cortes, 2015) applied a gain scheduling controller to a dual TRUAV. Based on the Jacobian linearisation of the model of the drone, a set of linear controllers was designed for takeoff, vertical, hovering, and horizontal flight conditions.

Govdeli et al. (Govdeli et al., 2019) presented a Quad-Tilt-Rotor with two configurations. The authors used a PID controller to generate the control inputs for the longitudinal plan. The parameters of the forward transition controller were different from those of the backward transition controller. The control scheme did not guarantee to maintain the altitude during the transition.

Chen et al. (Chen et al., 2021) designed Cascaded controller for a Three-Rotor TRUAV. During the transition, the drone was controlled by mixing control surfaces and rotors depending on the airspeed. A sliding mode controller was used for all channels.

To the best of the author's knowledge, all previous works employ two controllers for each flight phase. In this paper, a control architecture employing a single controller for both VTOL and cruise flight phases is considered. A sliding mode controller (SMC) is then derived to ensure trajectory tracking. The proposed solution is validated on the full nonlinear model of the famous Zagi wing drone.

The remainder of this paper is organised into four sections. Section II presents the development of the TRUAV's kinematic and dynamic model. The control architecture and associated sliding mode controller are discussed in section III. Obtained results are presented and analysed in section IV.

## 2 DYNAMIC MODELING OF THE Quad-TRUAV

The dynamic model of the Quad-TRUAV is derived based on the Newton-Euler formalism

$$\begin{aligned} m\dot{V}_g^E &= R_B^E F^B \\ \mathbf{I}\dot{\Omega} + \Omega \times \mathbf{I}\Omega &= M^B \end{aligned} \quad (1)$$

Using the blade element theory, the thrust and reactive torque generated by a rotor are modelled as (Prouty, 2002)

$$\begin{cases} T_i = K_l \cdot \omega_i^2 \\ C_i = K_c \cdot \omega_i^2 \end{cases} \quad (2)$$

with  $K_l$  and  $K_c$  the thrust and drag coefficients.

After development, the total thrust forces generated by the four rotors are expressed in the body frame as

$$F_r^B = \begin{bmatrix} F_{rx} \\ F_{ry} \\ F_{rz} \end{bmatrix} = \begin{bmatrix} T_{1+2}C\gamma_1 + T_{3+4}C\gamma_2 \\ 0 \\ -T_{1+2}S\gamma_1 - T_{3+4}S\gamma_2 \end{bmatrix} \quad (3)$$

where  $T_{1+2} = T_1 + T_2$  and  $T_{3+4} = T_3 + T_4$ .

The total moment generated by the four rotors is expressed w.r.t the body frame as

$$M_r^B = \begin{bmatrix} \tau_\phi \\ \tau_\theta \\ \tau_\psi \end{bmatrix} \quad (4)$$

with

$$M_r^B = \begin{bmatrix} (K_{ld}c\gamma_1 - l_y s\gamma_1)T_{1-2} + (K_{lc}\gamma_2 - l_y s\gamma_2)T_{3-4} \\ l_x T_{1+2} - l_x T_{3+4} \\ -(K_{ls}\gamma_1 + l_y c\gamma_1)T_{1-2} - (K_{ls}\gamma_2 + l_y c\gamma_2)T_{3-4} \end{bmatrix} \quad (5)$$

With  $T_{1-2} = T_1 - T_2$ ,  $T_{3-4} = T_3 - T_4$ ,  $l_x$  and  $l_y$  are the position coordinates of rotors, and  $K_{ld} = K_c/K_l$  denotes the constant of proportionality between the two drag and the thrust

Assuming a small angle of attack and that the airflow remains laminar and attached, the aerodynamic forces  $F_a = [L \ D \ f_y]$  and moments  $M_a = [l \ m \ n]$  expressed in the wind frame,  $R_w$ , can be approximated as (Beard and McLain, 2012)

$$\begin{aligned} L &= \frac{1}{2}\rho V_a^2 SC_L \\ D &= \frac{1}{2}\rho V_a^2 SC_D \\ f_y &= \frac{1}{2}\rho V_a^2 SC_y \end{aligned} \quad (6)$$

$$\begin{aligned} l &= \frac{1}{2}\rho V_a^2 Sbc_l \\ m &= \frac{1}{2}\rho V_a^2 ScC_m \\ n &= \frac{1}{2}\rho V_a^2 Sbc_n \end{aligned} \quad (7)$$

with  $V_a$  the resultant air mass velocity, calculated as the difference between the drone's ground speed and the wind speed:

$$V_a = V_g - V_{wind} \quad (8)$$

Parameter  $S$  refers to the wing area,  $c$  is the mean chord, and  $b$  is the wing span. The aerodynamic coefficients  $C_L$ ,  $C_D$  and  $C_m$  are respectively the lift, drag, and pitch moment coefficients for the longitudinal plan. For the lateral plan,  $C_y$ ,  $C_l$  and  $C_n$  are the lateral forces, roll and yaw moments coefficients. These parameters are approximated to (Beard and McLain, 2012)

$$\begin{aligned} C_L &= C_{L_0} + C_{L_\alpha} \alpha + C_{L_q} \frac{c}{2V_a} q \\ C_D &= C_{D_0} + C_{D_\alpha} \alpha + C_{D_q} \frac{c}{2V_a} q \\ C_m &= C_{m_0} + C_{m_\alpha} \alpha + C_{m_q} \frac{c}{2V_a} q \\ C_y &= C_{y_0} + C_{y_\beta} \beta + C_{y_p} \frac{b}{2V_a} p + C_{y_r} \frac{b}{2V_a} r \\ C_l &= C_{l_0} + C_{l_\beta} \beta + C_{l_p} \frac{b}{2V_a} p + C_{l_r} \frac{b}{2V_a} r \\ C_n &= C_{n_0} + C_{n_\beta} \beta + C_{n_p} \frac{b}{2V_a} p + C_{n_r} \frac{b}{2V_a} r \end{aligned} \quad (9)$$

with  $\alpha$  the angle of attack, and  $\beta$  the side slip angle.

After developing the total force and moment acting on the Quad-TRUAV, the dynamics of the translational motion of the drone are expressed w.r.t the inertial frame as

$$\begin{bmatrix} \ddot{x} \\ \ddot{y} \\ \ddot{z} \end{bmatrix} = \frac{1}{m} \cdot R_B^E \begin{bmatrix} T_{1+2} c \gamma + F_{ax} \\ F_{ay} \\ -T_{1+2} s \gamma - T_{3+4} + F_{az} \end{bmatrix} + \begin{bmatrix} 0 \\ 0 \\ g \end{bmatrix} \quad (10)$$

with  $F_{ax}$ ,  $F_{ay}$ , and  $F_{az}$  the aerodynamic forces expressed in the body frame. The rotational dynamics of the Quad-TRUAV are expressed w.r.t the body frame as

$$\begin{bmatrix} \dot{p} \\ \dot{q} \\ \dot{r} \end{bmatrix} = J^{-1} \left\{ - \begin{bmatrix} p \\ q \\ r \end{bmatrix} \times J \begin{bmatrix} p \\ q \\ r \end{bmatrix} + \begin{bmatrix} \tau_\phi + m_{ax} \\ \tau_\theta + m_{ay} \\ \tau_\psi + m_{az} \end{bmatrix} \right\} \quad (11)$$

with  $m_{ax}$ ,  $m_{ay}$ , and  $m_{az}$  the components of the aerodynamic moments expressed in the body frame. This gives, after development

$$\begin{bmatrix} \dot{p} \\ \dot{q} \\ \dot{r} \end{bmatrix} = \begin{bmatrix} I_1 p q + I_2 q r + I_3 (\tau_\phi + l_{az}) + I_4 (\tau_\psi + m_{ax}) \\ I_5 p r + I_6 ((r^2 - p^2) + \tau_\theta + m_{ay}) \\ I_7 p q + I_8 q r + I_4 (\tau_\phi + m_{az}) + I_9 (\tau_\psi + m_{ax}) \end{bmatrix} \quad (12)$$

with:

$$I_D = I_{xx} I_{zz} - I_{xz}^2, \quad (13)$$

$$I_1 = \frac{1}{I_D} (I_{xz} (I_{xx} - I_{yy} + I_{zz})), \quad (14)$$

$$I_2 = (I_{yy} I_{zz} - I_{xz}^2 - I_{zz}^2), \quad (15)$$

$$I_3 = \frac{I_{zz}}{I_D}, \quad (16)$$

$$I_4 = \frac{I_{xz}}{I_D}, \quad (17)$$

$$I_5 = \frac{(I_{zz} - I_{xx})}{I_{yy}}, \quad (18)$$

$$I_6 = \frac{I_{xz}}{I_{yy}}, \quad (19)$$

$$I_7 = \frac{1}{I_D} (I_{xx}^2 + I_{xz}^2 - I_{xx} I_{yy}), \quad (20)$$

$$I_8 = \frac{I_{xz}}{I_D} (I_{yy} - I_{xx} - I_{zz}), \quad (21)$$

$$I_9 = \frac{I_{xx}}{I_D}. \quad (22)$$

### 3 CONTROL SCHEME & SMC DESIGN

The control scheme adopted in this work is outlined in Fig.2. Unlike conventional quadrotors our Quad-TRUAV has an extra control input, which is the tilt angle of the front rotors. In our control scheme, this input is exploited to decouple the forward position control from that of the pitch angle. The TRUAV's trajectory is, thus, specified by five independent variables: the 3D position  $(x_d, y_d, z_d)$ , as well as the pitch and yaw angles  $(\theta_d, \psi_d)$ .

In our control scheme, the output of the forward position controller,  $U_x$ , is mapped to the tilt angle  $\gamma$ . The loss in vertical thrust force caused by the tilting of the front rotors is compensated for by raising the rotation speed of these rotors such that the projection of the generated forces on the  $z$  axis meets the control output of the altitude controller,  $U_z$ .

The virtual control output  $U_y$  is mapped to the roll angle  $\phi$  in the same way as it is in a conventional multirotor. The heading angle,  $\psi$ , is also controlled like a conventional multi-rotor. The pitch angle controller, on the other hand, takes into account the variation in the tilt angle of the front rotors.

To simplify the controller design, the following assumptions are considered:

- The roll  $\phi$  and pitch  $\theta$  angles are small, so Euler angle rate are approximated to the angular rates in the body frame

$$\begin{bmatrix} \dot{\phi} \\ \dot{\theta} \\ \dot{\psi} \end{bmatrix} = \begin{bmatrix} p \\ q \\ r \end{bmatrix} \quad (23)$$

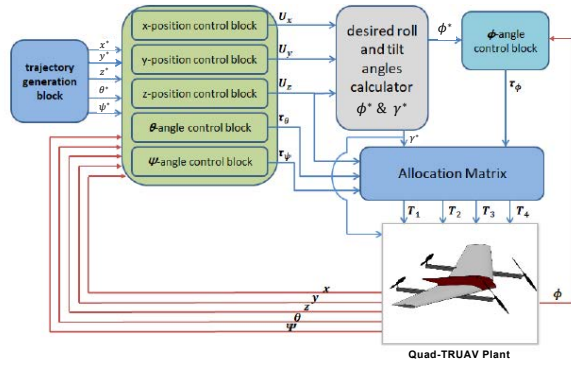


Figure 2: Proposed Control scheme of the Quad-TRUAV.

- Given the symmetry of the Quad-TRUAV, the term  $I_{xz}$  in the inertia matrix is neglected. This simplifies equation (12) to

$$\begin{bmatrix} \ddot{\phi} \\ \ddot{\theta} \\ \ddot{\psi} \end{bmatrix} = \begin{bmatrix} \frac{I_{yy}-I_{zz}}{I_{xx}}\dot{\theta}\dot{\psi} + \frac{\tau_{\phi}+l}{I_{xx}} \\ \frac{I_{zz}-I_{xx}}{I_{yy}}\dot{\phi}\dot{\psi} + \frac{\tau_{\theta}+m}{I_{yy}} \\ \frac{I_{xx}-I_{yy}}{I_{zz}}\dot{\phi}\dot{\theta} + \frac{\tau_{\psi}+n}{I_{zz}} \end{bmatrix} \quad (24)$$

The control input vector is chosen as

$$U = [ U_1 \quad U_2 \quad \tau_{\phi} \quad \tau_{\theta} \quad \tau_{\psi} ] \quad (25)$$

with

$$U_1 = -T_{1+2} \sin \gamma - T_{3+4} \quad (26)$$

$$U_2 = T_{1+2} \cos \gamma \quad (27)$$

$$\tau_{\phi} = (K_{ld} \cos \gamma - l_y \sin \gamma) T_{1-2} - l_y T_{3-4} \quad (28)$$

$$\tau_{\theta} = \sin \gamma l_x T_{1+2} - l_x T_{3+4} \quad (29)$$

$$\tau_{\psi} = -(K_{ld} \sin \gamma + l_y \cos \gamma) T_{1-2} + K_{ld} T_{3-4} \quad (30)$$

The corresponding allocation matrix is

$$M = \begin{bmatrix} -(s\theta c\gamma + c\theta c\phi s\gamma) & -c\theta c\phi & 0 & 0 \\ 0 & 0 & (K_{ld} c\gamma - l_y s\gamma) & -l_y \\ s\gamma l_x & -l_x & 0 & 0 \\ 0 & 0 & -(K_{ld} s\gamma + l_y c\gamma) & K_{ld} \end{bmatrix} \quad (31)$$

The thrust forces are hence calculated as

$$\begin{bmatrix} T_{1+2} \\ T_{3+4} \\ T_{1-2} \\ T_{3-4} \end{bmatrix} = M^{-1} \begin{bmatrix} U_z \\ \tau_{\phi} \\ \tau_{\theta} \\ \tau_{\psi} \end{bmatrix} \quad (32)$$

For the sake of clarity, the following intermediate control variables are considered

$$U_x = c\psi c\theta \cdot U_2 + (c\psi s\theta c\phi + s\psi s\phi) U_1 \quad (33)$$

$$U_y = s\psi c\theta \cdot U_2 + (c\phi s\theta s\psi - s\phi c\psi) U_1 \quad (34)$$

$$U_z = -s\theta U_2 + (c\phi c\theta) U_1 \quad (35)$$

In what follows, we present the design of an SMC controller for each variable of the Quad-TRUAV. Sliding mode control belongs to the family of discontinuous control systems. It is an ideal instrument for addressing the control of complex dynamic plants, such as that of the Quad-TRUAV.

We start with the design of the roll angle controller. The tracking error of the roll angle is defined as,

$$e_{\phi} = \phi^* - \phi \quad (36)$$

The corresponding sliding surface is chosen such that

$$\sigma_{\phi} = \dot{e}_{\phi} + \lambda_{\phi} e_{\phi} \quad (37)$$

with  $\lambda_{\phi} > 0$ .

This gives the following derivative for the sliding surface:

$$\dot{\sigma}_{\phi} = \ddot{e}_{\phi} + \lambda_{\phi} \dot{e}_{\phi} \quad (38)$$

$$= \ddot{\phi}^* - \ddot{\phi} + \lambda_{\phi} (\dot{\phi}^* - \dot{\phi}) \quad (39)$$

A Lyapunov function,  $V$ , is then chosen, such that

$$V = \frac{1}{2} \sigma_{\phi}^2 \quad (40)$$

To ensure the sliding condition we have

$$\dot{\sigma}_{\phi} = -\eta_{\phi} \text{sign}(\sigma_{\phi}) \quad (41)$$

with  $\eta_{\phi} > 0$ .

By deriving the sliding surface in equation (39) and replacing  $\dot{\phi}$  by its definition from equation (24), the control input  $\tau_{\phi}$  of the SMC controller is obtained as

$$\tau_{\phi} = \frac{1}{b_1} (-a_1 \dot{\theta} \dot{\psi} - b_1 l + \ddot{\phi}^* + \lambda_{\phi} (\dot{\phi}^* - \dot{\phi}) + \eta_{\phi} \text{sign} \sigma_{\phi}) \quad (42)$$

with  $\eta_{\phi} > 0$ .

Following the same steps as for the roll controller, the control inputs for the pitch angle  $\tau_{\theta}$ , the heading angle  $\tau_{\psi}$ , and the 3D position  $U_z$ ,  $U_x$ , and  $U_y$  are calculated as

$$\tau_{\theta} = \frac{1}{b_2} (-a_2 \dot{\phi} \dot{\psi} - b_2 m + \ddot{\theta}^* + \lambda_{\theta} (\dot{\theta}^* - \dot{\theta}) + \eta_{\theta} \text{sign} \sigma_{\theta}) \quad (43)$$

$$\tau_{\psi} = \frac{1}{b_3} (-a_3 \dot{\phi} \dot{\theta} - b_3 n + \ddot{\psi}^* + \lambda_{\psi} (\dot{\psi}^* - \dot{\psi}) + \eta_{\psi} \text{sign} \sigma_{\psi}) \quad (44)$$

$$U_z = m \left( -g - \frac{F_{az}^i}{m} + \ddot{z}^* + \lambda_z (z^* - z) + \eta_z \text{sign} \sigma_z \right) \quad (45)$$

$$U_x = m \left( -\frac{F_{ax}^i}{m} + \ddot{x}^* + \lambda_x (x^* - x) + \eta_x \text{sign} \sigma_x \right) \quad (46)$$

$$U_y = m \left( -\frac{F_{ay}^i}{m} + \ddot{y}^* + \lambda_y (y^* - y) + \eta_y \text{sign} \sigma_y \right) \quad (47)$$

with  $\eta_{\theta}$ ,  $\eta_{\psi}$ ,  $\eta_z$ ,  $\eta_x$  and  $\eta_y$  real positive parameters.

Table 1: Parameters of the Zagi flying wing used in this work.

Parameter	Value	Longitudinal Coef.		Lateral Coef.	
		Value	Value	Value	Value
$m$	1.56 kg	$CL_0$	0.09167	$CY_0$	0
$I_{xx}$	0.1147 kg $m^2$	$CD_0$	0.01631	$Cl_0$	0
$I_{yy}$	0.0576 kg $m^2$	$Cm_0$	-0.02338	$Cn_0$	0
$I_{zz}$	0.1712 kg $m^2$	$CL_\alpha$	3.5016	$CY_\beta$	-0.07359
$I_{xz}$	0.0015 kg $m^2$	$CD_\alpha$	0.2108	$Cl_\beta$	-0.02854
$S$	0.2589 $m^2$	$Cm_\alpha$	-0.5675	$Cn_\beta$	-0.00040
$b$	1.4224 m	$CL_q$	2.8932	$CY_p$	0
$c$	0.3302 m	$CD_q$	0	$Cl_p$	-0.3209
$\rho$	1.2682 kg/ $m^3$	$Cm_q$	-1.3990	$Cn_p$	-0.01297
				$CY_r$	0
				$Cl_r$	0.03066
				$Cn_r$	-0.00434

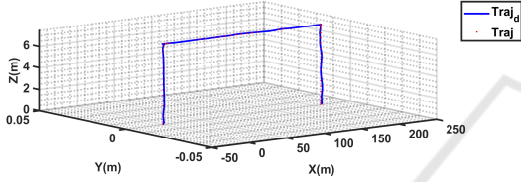


Figure 3: 3D trajectory followed by the Quad-TRUAV.

## 4 SIMULATION RESULTS AND DISCUSSION

To validate the proposed control scheme and the associated SMC controller, simulations are conducted on the full non-linear model of the Quad-TRUAV. The model considered in this work is that of the famous Zagi flying wing (Beard and McLain, 2012). The geometrical, inertial, and aerodynamic parameters of this drone are summarised in table 1.

We consider the saturation of the four actuators to make our model even more realistic. The saturation is selected so that the four rotors can only provide a lift force equal to double the drone's weight. The trajectory under consideration contains three segments. The initial phase consists of a takeoff and ascent to a height of 7.5 meters. During the second phase, the drone pitches up and speeds forward until it reaches 7 m/s, which it sustains for 20 seconds. The drone then begins to decelerate until it comes to a stop, levels out, and begins to land.

Fig.3 depicts the 3D reference trajectory and the trajectory followed by the drone. As the figure shows, the proposed control scheme and associated sliding mode controller were capable of smoothly tracking the reference trajectory in all its phase. This solution also ensured a smooth transition, between VTOL and fixed wing mode.

Fig. 4a shows in more detail the temporal variation of the 3D trajectory followed by the drone and the corresponding tracking errors. The tracking errors along the  $x$  axis are much higher compared to the  $y$  and  $z$  axes. This is due to the higher manoeuvres that the drone makes along this axis.

Fig. 5 plots the evolution of the drone's attitude in terms of Euler angles. It is to note that the variations of the pitch angle at 25 sec and 70 sec did not affect the drone's position despite the coupling between the  $x$  position and pitch angle. This is achieved thanks to the non-linearity of the SMC controller, which explicitly compensates for this coupling.

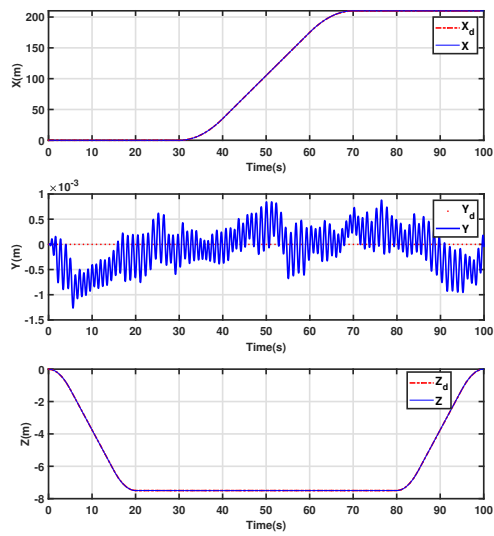
With regard to the control efforts, the thrust forces generated by the four rotors are depicted in Fig. 6a. As the drone moves forward, its wings generate more lift and less thrust is needed to maintain its altitude.

The average value of the rotors' thrust is about 4N in the VTOL phase. This value is decreased to about 2.5N in the cruise flight phase. This results in less power consumption and hence more endurance as mentioned earlier.

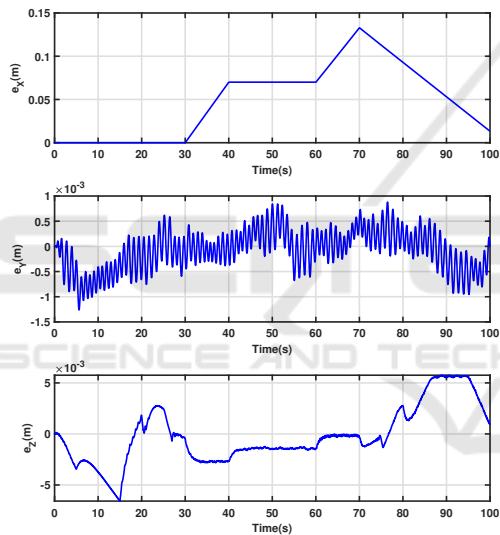
The main drawback of the SMC controller is the chattering which appears in all the control inputs. This effect would be less pronounced in practice, because it will be filtered by the actuators' dynamics.

Fig. 6b shows the evolution of the tilting angle. The pitch up action, which happens at 25 sec, results in a decrease of the tilt angle by about  $70^\circ$ . During the transition, the tilt angle continues to decrease to about  $60^\circ$ .

From these results, it is concluded that all control inputs remain within the saturation limits we set for them. The maximum tilt angle achieved was about  $48^\circ$  from vertical, while its saturation was set to  $60^\circ$ . It is worth noting that this saturation is necessary for the Quad-TRUAV, since a minimum component of



(a)



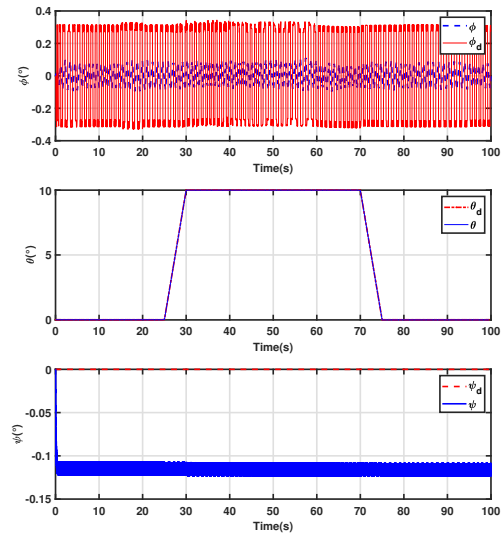
(b)

Figure 4: Trajectory tracking results: (a) desired and actual horizontal positions and altitude; (b) corresponding tracking errors.

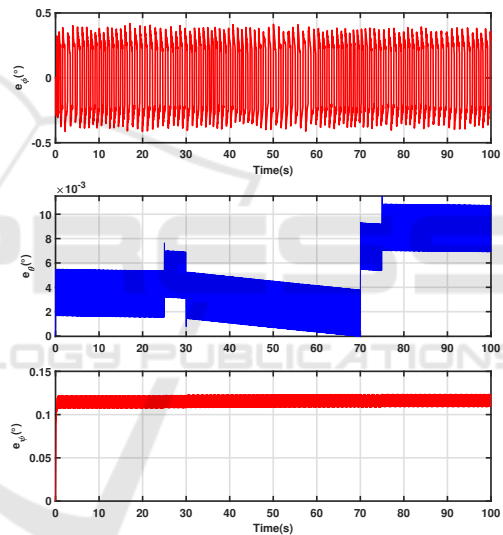
thrust on the  $z_b$  is required to allow the control of the pitch angle.

## 5 CONCLUSION

This paper dealt with the problem of trajectory tracking for a tilt-rotor convertible UAV. Since the drone contains no control surfaces, only rotors were relied on to ensure the control of its 6 DOF. A control scheme which takes into account this particularity and a sliding mode controller were designed to ensure trajectory tracking.



(a)



(b)

Figure 5: Evolution of the drone's attitude : (a) From top to bottom roll, pitch, and yaw angles (b) corresponding tracking errors.

The proposed control scheme and associated SMC were validated on the full non-linear model of the drone, including all couplings and actuators saturation. Simulation results were very promising. Future works will investigate solutions for the estimation of the aerodynamic forces and moments and the implementation of the proposed control solution on a real platform.

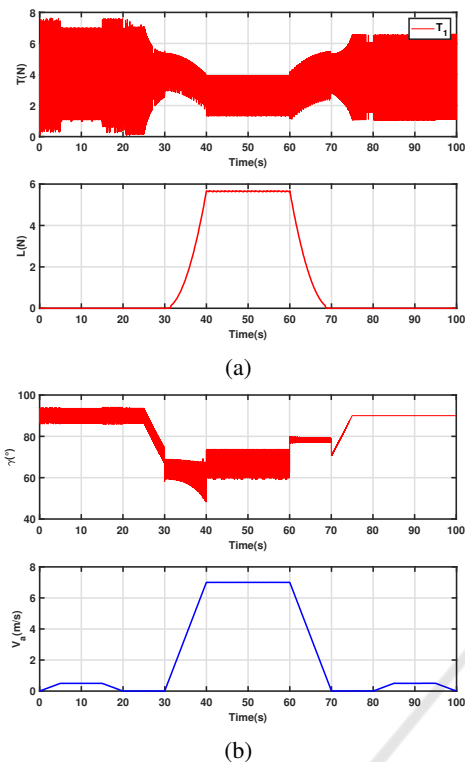


Figure 6: Control inputs: (a) thrust and lift forces; (b) tilt angle and airspeed.

## REFERENCES

- Beard, R. W. and McLain, T. W. (2012). *Small Unmanned Aircraft Theory and Practice*. Princeton University Press.
- Chen, C., Zhang, J., Wang, N., Shen, L., and Li, Y. (2021). Conversion control of a tilt tri-rotor unmanned aerial vehicle with modeling uncertainty. *International Journal of Advanced Robotic Systems*, 18:172988142110270.
- Ducard, G. J. and Allenspach, M. (2021). Review of designs and flight control techniques of hybrid and convertible vtol uavs. *Aerospace Science and Technology*, 118:107035.
- Flores, G. and Lozano, R. (2013). Transition flight control of the quad-tilting rotor convertible mav. pages 789–794. IEEE. a nonlinear control strategy based on saturations and Lyapunov design is given; stabilize the altitude  $z$  with a bounded control input, we will use the nested saturation control approach.
- Flores, G. R., Escareño, J., Lozano, R., and Salazar, S. (2012). Quad-tilting rotor convertible mav: Modeling and real-time hover flight control. *Journal of Intelligent & Robotic Systems*, 65:457–471.
- Govdéli, Y., Muzaffar, S. M. B., Raj, R., Elhadidi, B., and Kayacan, E. (2019). Unsteady aerodynamic modeling and control of pusher and tilt-rotor quadplane configurations. *Aerospace Science and Technology*, 94:105421.
- Hegde, N. T., George, V., Nayak, C. G., and Kumar, K. (2019). Design, dynamic modelling and control of tilt-rotor uavs: a review. *International Journal of Intelligent Unmanned Systems*, 8:143–161.
- Hernandez-Garcia, R. G. and Rodriguez-Cortes, H. (2015). Transition flight control of a cyclic tiltrotor uav based on the gain-scheduling strategy. pages 951–956. IEEE.
- Kim, J., Kim, S., Ju, C., and Son, H. I. (2019). Unmanned aerial vehicles in agriculture: A review of perspective of platform, control, and applications. *IEEE Access*, 7:105100–105115.
- Li, X., Tan, J., Liu, A., Vijayakumar, P., Kumar, N., and Alazab, M. (2021). A novel uav-enabled data collection scheme for intelligent transportation system through uav speed control. *IEEE Transactions on Intelligent Transportation Systems*, 22:2100–2110.
- Papachristos, C., Alexis, K., and Tzes, A. (2012). Towards a high-end unmanned tri-tiltrotor: design, modeling and hover control. pages 1579–1584. IEEE.
- Papachristos, C., Alexis, K., and Tzes, A. (2013). Linear quadratic optimal trajectory-tracking control of a longitudinal thrust vectoring-enabled unmanned tri-tiltrotor. *IECON Proceedings (Industrial Electronics Conference)*, pages 4174–4179.
- Phung, D.-K. and Morin, P. (2014). Control of a new convertible uav with a minimal sensor suite. volume 2015-Febru, pages 229–235. IEEE.
- Prouty, R. W. (2002). *Helicopter Performance, Stability and Control*.
- Saeed, A. S., Younes, A. B., Cai, C., and Cai, G. (2018). A survey of hybrid unmanned aerial vehicles. *Progress in Aerospace Sciences*, 98:91–105.
- Saeed, A. S., Younes, A. B., Islam, S., Dias, J., Seneviratne, L., and Cai, G. (2015). A review on the platform design, dynamic modeling and control of hybrid uavs. pages 806–815. IEEE.
- Shakhtrah, H., Sawalmeh, A. H., Al-Fuqaha, A., Dou, Z., Almaita, E., Khalil, I., Othman, N. S., Khreishah, A., and Guizani, M. (2019). Unmanned aerial vehicles (uavs): A survey on civil applications and key research challenges. *IEEE Access*, 7:48572–48634.
- Su, J., Su, C., Xu, S., and Yang, X. (2019). A multi-body model of tilt-rotor aircraft based on kane’s method. *International Journal of Aerospace Engineering*, 2019:1–10.
- Ta, D. A., Fantoni, I., and Lozano, R. (2012). Modeling and control of a tilt tri-rotor airplane. pages 131–136. IEEE. This paper is used to cite the works used for controlling TRUAV.